

# Quantum stabilization of classically unstable plateau structures

Tommaso Coletta,<sup>1</sup> M. E. Zhitomirsky,<sup>2</sup> and Frédéric Mila<sup>1</sup>

<sup>1</sup>*Institute of Theoretical Physics, Ecole Polytechnique Fédérale de Lausanne (EPFL), CH-1015 Lausanne, Switzerland*

<sup>2</sup>*Service de Physique Statistique, Magnétisme et Supraconductivité, UMR-E9001 CEA-INAC/UJF, 17 rue des Martyrs, F-38054 Grenoble, France*  
(Dated: December 14, 2012)

Motivated by the intriguing report, in some frustrated quantum antiferromagnets, of magnetization plateaus whose simple collinear structure is *not* stabilized by an external magnetic field in the classical limit, we develop a semiclassical method to estimate the zero-point energy of collinear configurations even when they do not correspond to a local minimum of the classical energy. For the spin-1/2 frustrated square-lattice antiferromagnet, this approach leads to the stabilization of a large 1/2 plateau with “up-up-up-down” structure for  $J_2/J_1 > 1/2$ , in agreement with exact diagonalization results, while for the spin-1/2 anisotropic triangular antiferromagnet, it predicts that the 1/3 plateau with “up-up-down” structure is stable far from the isotropic point, in agreement with the properties of  $\text{Cs}_2\text{CuBr}_4$ .

**Introduction.**—Frustration is responsible for the emergence of several remarkable properties in quantum magnets, ranging from rather exotic types of order such as quadrupolar or nematic order to resonating valence bond or algebraic spin liquids [1]. In the presence of an external field, frustration is also known to be at the origin of several types of accidents in the magnetization curve, including kinks, jumps and plateaus. Of all these remarkable features, magnetization plateaus at rational value of the magnetization are probably the best documented ones experimentally, and their theory is likewise quite advanced. Following the terminology of Hida and Affleck [2], two kinds of plateaus have been identified [3]: ‘classical’ plateaus [4–6], whose structure has a simple classical analog with spins up or down along the external field, and ‘quantum’ plateaus [7–11], which have no classical analog and correspond to a Wigner crystal of triplets in a sea of singlets. In the case of quantum plateaus, the mechanism is clear: frustration reduces the kinetic energy of triplets, resulting in a crystallization at commensurate densities. The main open problem is to be predictive for high commensurability plateaus since it requires a precise knowledge of the long-range part of the triplet-triplet interaction.

By contrast, and somehow surprisingly, the theory of classical plateaus is not complete yet. The paradigmatic example of a classical plateau is the 1/3 magnetization plateau of the Heisenberg antiferromagnet on a triangular lattice, studied by Chubukov and Golosov [5] in the context of a  $1/S$  expansion. In this system the three sublattice up-up-down (*uud*) structure appears classically at  $H = H_{\text{sat}}/3$ , and quantum fluctuations stabilize this *uud* state in a finite field range around  $H_{\text{sat}}/3$ , leading to the 1/3 plateau. The basic qualitative idea in the spirit of the order by disorder is that collinear configurations often have a softer spectrum and, hence, a smaller zero-point energy [12, 13]. The prediction of the 1/3 plateau has been confirmed by exact diagonalization of finite clusters for  $S = 1/2$  and 1 [14], and the theory of Chubukov and Golosov can be extended to all cases where a collinear state is classically stabilized for a certain field.

There are cases, however, where a classical plateau has been suggested to exist although the collinear structure sta-

bilized for quantum spins is *not* the ground state for classical spins, the classical ground state in the appropriate field range being in general a non-coplanar structure. This is for instance the case of the spin-1/2  $J_1$ – $J_2$  model on the square lattice, for which exact diagonalizations have revealed the presence of a four sublattice up-up-up-down (*uuud*) 1/2 plateau in a parameter range where the classical ground state has a canted stripe structure (see below). Another example is the 1/3 plateau of the Heisenberg model on the anisotropic triangular lattice, a model relevant to the compound  $\text{Cs}_2\text{CuBr}_4$ . To develop a general theory of classical plateaus in that situation remains the main open issue in the field.

The goal of this Letter is to develop such a theory. For that purpose, we start with a general Heisenberg model in an external field defined by the spin Hamiltonian

$$\mathcal{H} = \sum_{\langle i,j \rangle} J_{ij} \mathbf{S}_i \cdot \mathbf{S}_j - H \sum_i S_i^z, \quad (1)$$

and show how to estimate the zero-point energy of collinear states *even if they do not minimize the classical energy*. More precisely, we derive an upper bound of this energy to order  $1/S$ . If the energy of a collinear state estimated in this way is lower than that of the classical ground state (including the zero-point energy), then the collinear state must be the ground state since the energy used for the comparison is an *upper bound*. Correspondingly, the quantum antiferromagnet exhibits a magnetization plateau in a certain field range, which may generally exceed our conservative theoretical estimate based on the upper energy-bound. We apply this approach to the  $J_1$ – $J_2$  model on a square lattice and to the Heisenberg antiferromagnet on the anisotropic triangular lattice, with results in remarkable agreement with existing numerical data for  $S = 1/2$ .

**General formalism.**—We propose a simple method to test for the stability of plateau structures in the framework of the linear spin-wave theory. First of all, we note that, since plateau structures are collinear, the fluctuation Hamiltonian around such structures in terms of Holstein-Primakoff bosons does not contain linear bosonic terms, and that the first relevant terms in its  $1/S$  expansion are quadratic. Since plateau

structures are classical minima of the energy only at specific values of couplings and magnetic field (if any) the corresponding harmonic fluctuation Hamiltonians are positive definite only at these specific points. Away from such points the correction to the classical energy cannot be straightforwardly computed. The fact that the spectrum is not well defined stems from the harmonic approximation. If the plateau state is to become the true quantum ground state, higher order terms in the spin-wave expansion must produce an excitation spectrum with positive frequencies. This approach requires to calculate nonlinear quantum corrections to the spectrum as done in Ref. [5] and in more recent studies [15, 16]. This is a rather cumbersome procedure, and it would be useful to have a simpler approach to determine if there is a plateau, and to estimate its width to the lowest-order in  $1/S$ . Besides, the calculation of the excitation spectrum for the plateau region allows to identify only second-order transitions, while in many experimental and model examples the transitions at the plateau boundaries are of the first-order and, therefore, require a full energetic comparison.

The proposed method to obtain a well-defined spectrum around a state which is not a classical ground state consists in adding a staggered-field term

$$\hat{V} = \delta \sum_i (S - S_i^z) \quad (2)$$

to the harmonic Hamiltonian. A similar approach has been introduced in a different context in [17, 18]. On each lattice site  $i$ , the staggered field  $\delta > 0$  is oriented in the direction  $\hat{z}_i$  of the corresponding classical spin. The extra term (2) amounts to a shift of the chemical potential of the Holstein-Primakoff bosons  $\hat{V} = \delta \sum_i a_i^\dagger a_i$  and yields a positive contribution to the spin-wave Hamiltonian. The magnitude of  $\delta$  is adjusted to ensure that the harmonic Hamiltonian is positive definite. The resulting spectrum obtained with the help of the Bogolyubov transformation has real and positive frequencies. The advantages of this variational approach are the following: the addition of  $\hat{V}$  to the Hamiltonian does not change the classical energy of the trial state and allows to obtain physically meaningful dispersion relations. Furthermore, since the expectation value of  $\hat{V}$  is strictly positive, the computed energy correction provides an *upper* bound for the energy of the plateau state. It should be noted that the suggested method is valid not only for collinear spin structures but can be extended to all structures that are saddle points of the classical energy, see [17, 18] and below.

**$J_1$ - $J_2$  model.**—For the frustrated square-lattice antiferromagnet the exchange interaction constants are  $J_{ij} = J_1$  and  $J_2$  for nearest and second-nearest neighbors, respectively. In zero field the classical ground state of the model is a helix with the ordering wave vector given by the minimum of the Fourier transform of the coupling interaction  $J_{\mathbf{q}} = 4J_1\gamma_{\mathbf{q}} + 4J_2\eta_{\mathbf{q}}$  with  $\gamma_{\mathbf{q}} = (\cos q_x + \cos q_y)/2$  and  $\eta_{\mathbf{q}} = \cos q_x \cos q_y$ . For  $J_2/J_1 < 1/2$ , the minimum corresponds to  $\mathbf{q}_N = (\pi, \pi)$ , i.e. to Néel order. In the opposite case  $J_2/J_1 > 1/2$ , the order by disorder mechanism selects collinear striped structures with

ordering wave vectors  $\mathbf{q}_S = (\pi, 0)$  or  $(0, \pi)$  [13]. The point  $J_2/J_1 = 1/2$  is highly degenerate since  $J_{\mathbf{q}}$  is minimal along the lines  $q_x = \pi$  and  $q_y = \pi$ . In the presence of a magnetic field both the Néel and the stripe structure are canted with a uniform spin component in the field direction. The canting angle  $\theta$  measured with respect to the  $z$  axis is given by  $\cos \theta_N = H/8J_1S$  and  $\cos \theta_S = H/(4J_1 + 8J_2)S$  for the two states.

The analysis of classical spin configurations in a magnetic field suggests the appearance of a  $1/2$ -magnetization plateau with a four-sublattice *uuud* structure for the strongly frustrated point  $J_2/J_1 = 1/2$  [6]. The conclusion has been supported by exact diagonalizations of finite clusters, though numerically the plateau extends well into the classically unstable region  $J_2/J_1 > 1/2$  with the largest width at  $J_2/J_1 \approx 0.6$ . Moreover, the linear spin-wave calculation for  $J_2/J_1 = 1/2$  shows that for this ratio of coupling constants the canted Néel state wins over the collinear plateau state [19] leaving an apparent problem with reconciling numerical and analytical results.

We now investigate the appearance of the  $1/2$ -magnetization plateau for the  $J_1$ - $J_2$  model using the variational harmonic theory outlined above. In the semiclassical approach deviations from the classical configuration are expressed as Holstein Primakoff bosons [20]. In the harmonic approximation the bosonic Hamiltonian can be split into three contributions:

$$\mathcal{H} = \mathcal{H}^{(0)} + \mathcal{H}^{(1)} + \mathcal{H}^{(2)}, \quad (3)$$

where  $\mathcal{H}^{(0)}$  is the classical energy of the system.  $\mathcal{H}^{(1)}$  and  $\mathcal{H}^{(2)}$  respectively contain only terms which are linear and quadratic in boson operators. The *uuud* state, being a collinear state, is such that no linear terms appear when performing the HP transformation, hence  $\mathcal{H}^{(1)} = 0$  for this state. In non collinear structures  $\mathcal{H}^{(1)}$  is proportional to the derivative of the classical energy with respect to spin orientations. It vanishes for the canted Néel and canted stripe structures over the entire parameter range since both are extrema of the classical energy. In fact the canted Néel (stripe) structure is a saddle point of the classical energy for  $H < H_{\text{sat}}$  and  $J_2/J_1 > 1/2$  (respectively  $J_2/J_1 < 1/2$ ).

The general structure of the quadratic bosonic Hamiltonian that describes harmonic fluctuations around these various configurations is given by

$$\mathcal{H} = NE_{\text{cl}} + \frac{1}{2} \sum_{\mathbf{k}} [\hat{\mathbf{a}}_{\mathbf{k}}^\dagger M_{\mathbf{k}} \hat{\mathbf{a}}_{\mathbf{k}} - \Delta_{\mathbf{k}}], \quad (4)$$

where  $E_{\text{cl}}$  is the classical energy per site of the state around which fluctuations are considered. For the canted Néel and the canted stripe states  $\hat{\mathbf{a}}_{\mathbf{k}}^\dagger = (a_{\mathbf{k}}^\dagger, a_{-\mathbf{k}})$  and  $M_{\mathbf{k}}$  is the  $2 \times 2$  matrix

$$M_{\mathbf{k}}(\mathbf{q}) = \begin{pmatrix} A_{\mathbf{k}}(\mathbf{q}) & B_{\mathbf{k}}(\mathbf{q}) \\ B_{\mathbf{k}}(\mathbf{q}) & A_{\mathbf{k}}(\mathbf{q}) \end{pmatrix}. \quad (5)$$

Coefficients  $A_{\mathbf{k}}(\mathbf{q})$  and  $B_{\mathbf{k}}(\mathbf{q})$  for Néel and striped structures

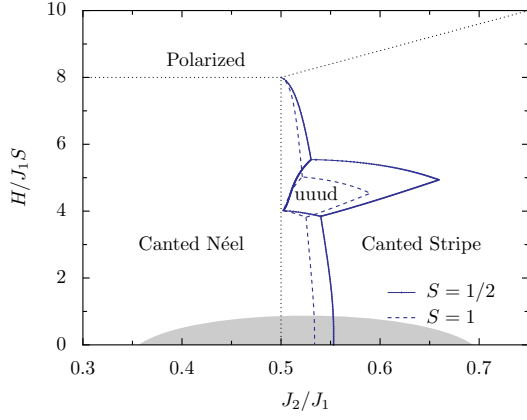


FIG. 1: Semiclassical phase diagram for the spin  $1/2$   $J_1 - J_2$  Heisenberg model in magnetic field. The  $uuud$  structure is stabilized by fluctuations over a wide parameter range. Dashed lines correspond to the phase diagram for  $S = 1$  and dotted lines to the classical phase boundaries. The shaded area represents schematically the gapped singlet phase for the spin- $1/2$  model.

are listed below:

$$\begin{aligned} A_{\mathbf{k}}(\mathbf{q}_N) &= 4J_1S(1 + \gamma_{\mathbf{k}} \cos^2 \theta_N) - 4J_2S(1 - \eta_{\mathbf{k}}), \\ B_{\mathbf{k}}(\mathbf{q}_N) &= -4J_1S\gamma_{\mathbf{k}} \sin^2 \theta_N \end{aligned} \quad (6)$$

and

$$\begin{aligned} A_{\mathbf{k}}(\mathbf{q}_S) &= 4J_2S(1 + \eta_{\mathbf{k}} \cos^2 \theta_S) + 2J_1S(\cos k_y + \cos^2 \theta_S \cos k_x), \\ B_{\mathbf{k}}(\mathbf{q}_S) &= -2S \sin^2 \theta_S (J_1 \cos k_x + 2J_2 \eta_{\mathbf{k}}) \end{aligned} \quad (7)$$

where we have used  $\mathbf{q}_S = (\pi, 0)$ . The additional constants  $\Delta_{\mathbf{k}}^N$  and  $\Delta_{\mathbf{k}}^S$  in Eq. (4) are given respectively by  $A_{\mathbf{k}}(\mathbf{q}_N)$  and  $A_{\mathbf{k}}(\mathbf{q}_S)$ .

The  $uuud$  state has a four-site unit cell, and  $\hat{\mathbf{a}}_{\mathbf{k}}^\dagger$  denotes  $(a_{1,\mathbf{k}}^\dagger, \dots, a_{4,\mathbf{k}}^\dagger, a_{1,-\mathbf{k}}, \dots, a_{4,-\mathbf{k}})$  with  $M_{\mathbf{k}}$  being the  $8 \times 8$  matrix obtained from (5) by substituting

$$A_{\mathbf{k}} = \begin{pmatrix} \bar{A}_{\mathbf{k}} & \bar{E}_{\mathbf{k}} & 0 & \bar{G}_{\mathbf{k}}^* \\ \bar{E}_{\mathbf{k}}^* & \bar{B}_{\mathbf{k}} & 0 & \bar{F}_{\mathbf{k}} \\ 0 & 0 & \bar{C}_{\mathbf{k}} & 0 \\ \bar{G}_{\mathbf{k}} & \bar{F}_{\mathbf{k}}^* & 0 & \bar{A}_{\mathbf{k}} \end{pmatrix}, \quad B_{\mathbf{k}} = \begin{pmatrix} 0 & 0 & -\bar{F}_{\mathbf{k}} & 0 \\ 0 & 0 & \bar{H}_{\mathbf{k}}^* & 0 \\ -\bar{F}_{\mathbf{k}}^* & \bar{H}_{\mathbf{k}} & 0 & -\bar{E}_{\mathbf{k}} \\ 0 & 0 & -\bar{E}_{\mathbf{k}}^* & 0 \end{pmatrix} \quad (8)$$

with coefficients

$$\begin{aligned} \bar{A}_{\mathbf{k}} &= -4J_2S + H, & \bar{B}_{\mathbf{k}} &= -4(J_1 - J_2)S + H, \\ \bar{C}_{\mathbf{k}} &= 4(J_1 + J_2)S - H, & \bar{E}_{\mathbf{k}} &= J_1S\tau_{k_y}, \\ \bar{F}_{\mathbf{k}} &= J_1S\tau_{k_x}, & \bar{G}_{\mathbf{k}} &= J_2S\tau_{-k_x}\tau_{-k_y}, & \bar{H}_{\mathbf{k}} &= -J_2S\tau_{-k_x}\tau_{k_y}, \end{aligned} \quad (9)$$

where  $\tau_k = (1 + e^{-i2k})$ . The constant  $\Delta_{\mathbf{k}}^{uuud}$  is given by  $2\bar{A}_{\mathbf{k}} + \bar{B}_{\mathbf{k}} + \bar{C}_{\mathbf{k}}$ . When the quadratic form of Eq. (4) is positive definite, it can be diagonalized by the standard Bogolyubov transformation allowing to compute the quantum corrections to the classical energy. For parameters for which the matrix  $M_{\mathbf{k}}$  is not positive definite we add to the Hamiltonian the term  $\hat{V}$  defined in Eq. (2). From the expression of  $\hat{V}$  in terms of HP

bosons it is clear that it leaves  $\mathcal{H}^{(0)}$  and  $\mathcal{H}^{(1)}$  unchanged while its effect on the bosonic Hamiltonian is to increase  $\Delta_{\mathbf{k}}$  and all diagonal elements of  $M_{\mathbf{k}}$  by  $\delta/2$ . The field  $\delta$  is adjusted to the minimal value which is sufficient to make  $M_{\mathbf{k}}$  positive definite over the entire Brillouin zone.

The phase diagram obtained by comparing the ground-state energies for three relevant spin structures is presented in Fig. 1 for  $S = 1/2$  and  $S = 1$ . The  $1/2$ -magnetization plateau is stabilized by quantum fluctuations over a wide range of parameters deep into the classically forbidden region  $J_2/J_1 > 1/2$ , though it remains energetically unfavorable at  $J_2/J_1 = 1/2$ . The width and position of the plateau are in good agreement with the exact diagonalization results of finite clusters with up to  $N = 36$  sites [6]. Figure 2 shows the magnetization curves for several ratios  $J_2/J_1$ . The magnetization curve for  $J_2/J_1 = 0.6$  with a large magnetization jump below the plateau and a much smaller anomaly above the plateau is in good correspondence with the numerical data for the same coupling ratio [6]. For  $J_2/J_1$  close to  $1/2$ , there is in addition a competition between the canted Néel and the canted stripe states. The Néel state has a softer spectrum than the stripe state and is stabilized beyond its classical boundary. This leads to an additional transition from the canted Néel state into the canted stripe structure which shows up as a small jump either above ( $J_2/J_1 = 0.525$ ) or below ( $J_2/J_1 = 0.55$ ) the  $1/2$ -plateau.

It should be pointed out that other states than those considered may be stabilized. One possible candidate, at the upper edge of the plateau, is the coplanar four sublattice state having three classical spins parallel and the remaining spin pointing in a different direction. This state can be naturally connected to the  $uuud$  state and is the analog of the state stabilized above the plateau in the isotropic triangular lattice. However, such a structure could not be investigated in our linear spin-wave approach since it is not a saddle point of the classical energy.

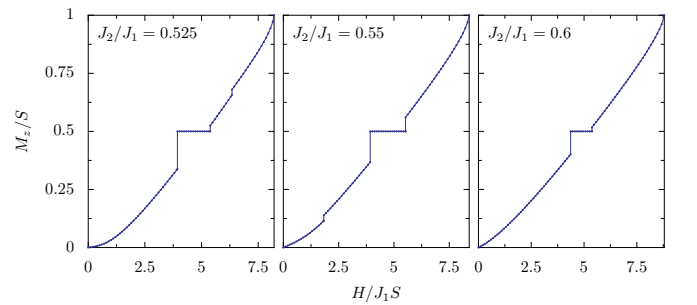


FIG. 2: Magnetization curves of the spin  $1/2$   $J_1 - J_2$  model for different ratios  $J_2/J_1$  obtained in the variational spin wave approach.

*Anisotropic triangular lattice.*—We now consider a second example of classically unstable magnetization plateau, the nearest-neighbor Heisenberg antiferromagnet on an orthorhombically distorted (anisotropic) triangular lattice. In this model spins are coupled by  $J_{ij} = J$  along horizontal chains and by  $J_{ij} = J'$  on zig-zag interchain bonds, see Fig 3(a). The spin- $1/2$  model is relevant for  $\text{Cs}_2\text{CuBr}_4$  [21–

[23], which has a  $1/3$  magnetization plateau although, with  $J' \sim 0.75J$ , it is quite far from the isotropic limit. The robustness of the *uud* plateau in the  $J$ – $J'$  model has been studied numerically [24] and analytically [15]. Nevertheless the extent of the plateau state around  $H/H_{\text{sat}} \sim 1/3$  and  $J'/J \sim 1$  and the nature of the states adjacent to the plateau region are still open questions. Furthermore, the stability method employed by Alicea *et al.* [15] allows to identify only second-order transitions out of the plateau state, while experiments typically find first-order transitions [23]. We shall see below that this fact finds a natural explanation in our theoretical approach.

The Fourier transform of the coupling interaction in the triangular-lattice, see Fig. 3(a), is given by  $J_{\mathbf{q}} = 2[J \cos \mathbf{q}\mathbf{a} + J' \cos \mathbf{q}\mathbf{b} + J' \cos \mathbf{q}(\mathbf{a} - \mathbf{b})]$ . In zero field the classical ground state is a helical spin structure whose ordering wavevector  $\mathbf{Q}$  minimizes  $J_{\mathbf{q}}$ . In the isotropic case  $J = J'$  this yields the well-known  $120^\circ$  spin structure. In the presence of a magnetic field the classical energy is minimized for canted helices or umbrella configurations, see Fig. 3(c), which have helical order in the  $xy$  plane and uniform spin component in the field direction. The canting angle of the helical structure measured with respect to the  $z$  axis is given by  $\cos \theta_H = H/(J_0 - J_{\mathbf{Q}})S$ . For the isotropic point  $J'/J = 1$  the canted helical state is degenerate with the coplanar Y- and V-type structures, see Fig. 3(b). Existing linear spin-wave calculations indicate that the coplanar structure is selected over the non coplanar one in the isotropic lattice and that the *uud* structure, classically stable at the field  $H_{\text{sat}}/3$ , is stabilized by fluctuations over a finite field range [5].

In the following we address the problem of the plateau stability for the anisotropic triangular lattice model by comparing ground-state energies for the canted helical state, the *uud* structure and the two 3-sublattice planar states as a function of  $J'/J$  and magnetic field. Away from  $J = J'$ , the 3-sublattice planar structures turn out to be, like the *uud*-state away from  $H_{\text{sat}}/3$  and  $J = J'$ , saddle points but not local minima of the classical energy, and to compute their zero-point energies, we use the variational spin-wave approach suggested above and add a staggered local field to the Hamiltonian [29].

The resulting phase diagram is shown in Fig. 4. The *uud* plateau state is stabilized well beyond the isotropic limit and extends over the range  $0.5 \lesssim J'/J \lesssim 1.5$ . Coplanar states are stabilized above and below the magnetization plateau with the exception of the plateau edges, where we find direct first-order

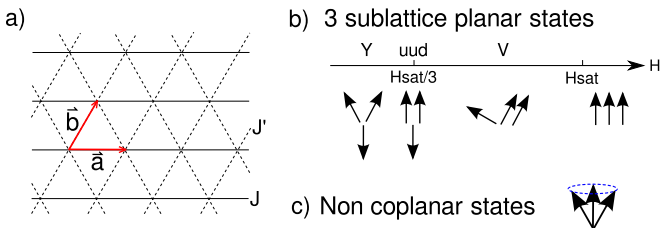


FIG. 3: a) Anisotropic triangular lattice and basis used in our calculations. b) 3-sublattice planar structure as a function of the magnetic field. c) Example of non coplanar canted helix.

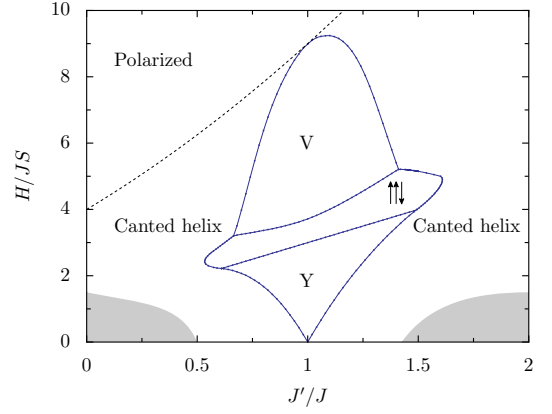


FIG. 4: Phase diagram of the spin-1/2 anisotropic triangular lattice in magnetic field. Y and V regions denote 3-sublattice planar states. The dashed line is the classical saturation field. The gray shading denotes regions where other phases than the canted helical states may be expected.

transitions from the *uud* state into the canted helical structure. From the energetic comparison it appears that the *uud* state does not extend into the Y-state region, so that the corresponding portion of the lower boundary of the plateau is perfectly linear (see Fig. 4). This is almost certainly an artefact of the method, which only gives an upper bound to the energy of the plateau, and the extent of the plateau is probably significantly larger. In fact, at  $J = J'$ , we obtain a plateau width which is only half that predicted in Refs. [5, 14]. We also note that the only coplanar states considered in our calculation are Y- and V-type structures, while for a substantial mismatch between  $J$  and  $J'$ , incommensurate coplanar structures may be also stabilized by quantum fluctuations. The variational spin-wave approach is not well-suited for treating them and we only remark that they may appear on the phase diagram at the expense of the canted helical structure. Finally, the gray shading in Fig. 4 indicates regions, where new quantum phases are expected. In fact, in zero field, theoretical and numerical approaches point to collinear spin correlations for weakly coupled chains, [25–27], while in the limit of strong interchain couplings the AFM Néel state should be stable down to  $J'/J \approx 1.5$  [27].

As compared to those of Alicea *et al.*, who also predicted an extended plateau region for small distortions  $[(1 - J'/J)^2 \lesssim 0.3]$  for the  $S = 1/2$  case [15], our results bring in a number of new insights. In the first place, the symmetry between  $J'/J < 1$  and  $J'/J > 1$  is lost. Second, a transition out of the plateau into the canted helical states is clearly present. Finally, for  $J'/J = 0.75$  relevant for  $\text{Cs}_2\text{CuBr}_4$  [21–23], we find a magnetization plateau width  $\Delta H/H_{\text{sat}} \approx 0.106$ , significantly larger than the experimental value  $\Delta H/H_{\text{sat}} \approx 0.052$  in  $\text{Cs}_2\text{CuBr}_4$ . Since in most cases our approach underestimates the plateau width, the difference must be due to additional effects not included in the anisotropic model, for instance the competition between quantum effects and Dzyaloshinskii-Moriya interactions [28].

**Conclusion.**—We have developed a general method to in-



investigate the stabilization of classical magnetization plateaus in cases where the corresponding configuration is not a minimum of the classical energy. This method is extremely simple since it only relies on the diagonalization of quadratic bosonic Hamiltonians and does not require to go beyond linear spin-wave theory, yet it appears to give remarkably accurate results, even for spin 1/2. This has been demonstrated in two cases of current interest, the  $J_1$ - $J_2$  Heisenberg model on the square lattice and the Heisenberg model on the anisotropic triangular lattice, for which it predicts that plateaus at magnetization 1/2 and 1/3 respectively are stabilized over a wide range of parameters.

We acknowledge useful discussions with Andrey Chubukov, Sergey Korshunov and Karlo Penc. This work has been supported by the Swiss National Fund and by MaNEP.

- 
- [1] C. Lacroix, P. Mendels, and F. Mila, eds., *Introduction to Frustrated Magnetism* (Springer, 2011).
  - [2] K. Hida and I. Affleck, J. Phys. Soc. Jpn. **74**, 1849 (2005).
  - [3] For a recent review, see M. Takigawa and F. Mila, *Magnetization Plateaus in Introduction to Frustrated Magnetism*, C. Lacroix, P. Mendels, F. Mila eds., p. 241 (Springer, 2011).
  - [4] H. Kawamura, J. Phys. Soc. Jpn. **53**, 2452 (1984).
  - [5] A. V. Chubukov and D. A. Golosov, J. Phys. Condens. Matter **3**, 69 (1991).
  - [6] M. E. Zhitomirsky, A. Honecker, and O. A. Petrenko, Phys. Rev. Lett. **85**, 3269 (2000).
  - [7] K. Totsuka, Phys. Rev. B **57**, 3454 (1998).
  - [8] F. Mila, Eur. Phys. J. B **6**, 201 (1998), ISSN 1434-6028.
  - [9] S. Miyahara and K. Ueda, Phys. Rev. Lett. **82**, 3701 (1999).
  - [10] J. Dorier, K. P. Schmidt, and F. Mila, Phys. Rev. Lett. **101**, 250402 (2008).
  - [11] A. Abendschein and S. Capponi, Phys. Rev. Lett. **101**, 227201 (2008).
  - [12] E. F. Shender, Sov. Phys. JETP **56**, 178 (1982).
  - [13] C. L. Henley, Phys. Rev. Lett. **62**, 2056 (1989).
  - [14] A. Honecker, J. Schulenburg, and J. Richter, J. Phys. Condens. Matter **16**, S749 (2004).
  - [15] J. Alicea, A. V. Chubukov, and O. A. Starykh, Phys. Rev. Lett. **102**, 137201 (2009).
  - [16] J. Takano, H. Tsunetsugu, and M. E. Zhitomirsky, J. Phys. Conf. Ser. **320**, 012011 (2011).
  - [17] T. Coletta, S. E. Korshunov, and F. Mila, To be published (2012).
  - [18] S. Wenzel, T. Coletta, S. E. Korshunov, and F. Mila, Phys. Rev. Lett. **109**, 187202 (2012).
  - [19] G. Jackeli and M. E. Zhitomirsky, Phys. Rev. Lett. **93**, 017201 (2004).
  - [20] T. Holstein and H. Primakoff, Phys. Rev. **58**, 1098 (1940).
  - [21] T. Ono, H. Tanaka, O. Kolomyiets, H. Mitamura, T. Goto, K. Nakajima, A. Oosawa, Y. Koike, K. Kakurai, J. Klenke, et al., J. Phys. Condens. Matter **16**, S773 (2004).
  - [22] H. Tsujii, C. R. Rotundu, T. Ono, H. Tanaka, B. Andraka, K. Ingersent, and Y. Takano, Phys. Rev. B **76**, 060406 (2007).
  - [23] N. A. Fortune, S. T. Hannahs, Y. Yoshida, T. E. Sherline, T. Ono, H. Tanaka, and Y. Takano, Phys. Rev. Lett. **102**, 257201 (2009).

- [24] S. Miyahara, K. Ogino, and N. Furukawa, Physica B **378B-380B**, 587 (2006).
- [25] O. A. Starykh and L. Balents, Phys. Rev. Lett. **98**, 077205 (2007).
- [26] A. Weichselbaum and S. R. White, Phys. Rev. B **84**, 245130 (2011).
- [27] J. Reuther and R. Thomale, Phys. Rev. B **83**, 024402 (2011).
- [28] C. Griset, S. Head, J. Alicea, and O. A. Starykh, Phys. Rev. B **84**, 245108 (2011).
- [29] See the supplemental material (below) for details concerning the spin wave calculation in the case of the anisotropic triangular lattice AFM

### SUPPLEMENTAL MATERIAL: LINEAR SPIN WAVE THEORY FOR THE ANISOTROPIC TRIANGULAR LATTICE AFM IN A MAGNETIC FIELD

The general structure of the bosonic fluctuation Hamiltonian around a given classical state is given in Eq. (4) of the main text. In this supplemental material we present the specific expressions for the canted helical state, the *uud* state and the 3- sublattice coplanar structures.

*Canted helical state* — The classical energy per site of the canted helical state expressed as a function of the canting angle  $\theta$  is given by

$$E_{\text{cl}}^H = S^2(J_0 \cos^2 \theta + J_Q \sin^2 \theta)/2 - HS \cos \theta. \quad (10)$$

It is minimal for  $\cos \theta^H = H/(J_0 - J_Q)S$ . The term  $\hat{\mathbf{a}}_{\mathbf{k}}^\dagger$  in Eq. (4) of the main text denotes  $(a_{\mathbf{k}}^\dagger, a_{-\mathbf{k}})$  and  $M_{\mathbf{k}}$  is the  $2 \times 2$  matrix

$$M_{\mathbf{k}}(\mathbf{Q}) = \begin{pmatrix} A_{\mathbf{k}}(\mathbf{Q}) + C_{\mathbf{k}}(\mathbf{Q}) & B_{\mathbf{k}}(\mathbf{Q}) \\ B_{\mathbf{k}}(\mathbf{Q}) & A_{\mathbf{k}}(\mathbf{Q}) - C_{\mathbf{k}}(\mathbf{Q}) \end{pmatrix} \quad (11)$$

with coefficients

$$\begin{aligned} A_{\mathbf{k}}(\mathbf{Q}) &= S \left( -J_Q + \frac{1}{4}(\cos^2 \theta + 1)(J_{\mathbf{k}+\mathbf{Q}} + J_{\mathbf{k}-\mathbf{Q}}) + \frac{1}{2} \sin^2 \theta J_{\mathbf{k}} \right), \\ B_{\mathbf{k}}(\mathbf{Q}) &= S \left( \frac{1}{4}(\cos^2 \theta - 1)(J_{\mathbf{k}+\mathbf{Q}} + J_{\mathbf{k}-\mathbf{Q}}) + \frac{1}{2} \sin^2 \theta J_{\mathbf{k}} \right), \\ C_{\mathbf{k}}(\mathbf{Q}) &= S \cos \theta (J_{\mathbf{k}+\mathbf{Q}} - J_{\mathbf{k}-\mathbf{Q}})/2. \end{aligned} \quad (12)$$

The additional term  $\Delta_{\mathbf{k}}$  in Eq. (4) of the main text is given by  $\Delta_{\mathbf{k}} = -S J_Q$ .

*3-sublattice coplanar states* — The classical energy per site of any 3- sublattice coplanar structure is given by

$$\begin{aligned} E_{\text{cl}}^{\text{coplanar}} &= S^2(J + 2J')(\cos \alpha_{1,2} + \cos \alpha_{1,3} + \cos \alpha_{2,3})/3 \\ &\quad - S H(\cos \alpha_1 + \cos \alpha_2 + \cos \alpha_3)/3 \end{aligned} \quad (13)$$

where  $\alpha_{i,j} = \alpha_i - \alpha_j$  are the spin orientations measured with respect to the field direction. The angles  $\alpha_i$  minimizing Eq. (13) are given by

$$\alpha_1^Y = \pi, \quad \cos \alpha_2^Y = \frac{1}{2} \left( \frac{H}{H_{\text{sat}}/3} + 1 \right), \quad \alpha_3^Y = -\alpha_2^Y \quad (14)$$

for  $0 \leq H \leq H_{\text{sat}}/3$  and

$$\begin{aligned} \cos \alpha_1^V &= \frac{H}{2H_{\text{sat}}} \left( 3 - \frac{H_{\text{sat}}^2}{H^2} \right), \\ \cos \alpha_2^V &= \cos \alpha_3^V = \frac{H}{4H_{\text{sat}}} \left( 3 + \frac{H_{\text{sat}}^2}{H^2} \right) \end{aligned} \quad (15)$$

for fields in the range  $H_{\text{sat}}/3 \leq H \leq H_{\text{sat}}$ , where  $H_{\text{sat}}$  is the saturation field  $H_{\text{sat}} = 3(J + 2J')S$ .

Since the states considered have three sites per unit cell the term  $\hat{\mathbf{a}}_{\mathbf{k}}^\dagger$  in Eq. (4) of the main text denotes  $(a_{\mathbf{k},1}^\dagger, a_{\mathbf{k},2}^\dagger, a_{\mathbf{k},3}^\dagger, a_{-\mathbf{k},1}, a_{-\mathbf{k},2}, a_{-\mathbf{k},3})$  and  $M_{\mathbf{k}}$  is the  $6 \times 6$  matrix

$$M_{\mathbf{k}}^{\text{Y,V}} = \begin{pmatrix} A & D_{\mathbf{k}}^* & H_{\mathbf{k}}^* & 0 & E_{\mathbf{k}}^* & I_{\mathbf{k}}^* \\ D_{\mathbf{k}} & B & F_{\mathbf{k}}^* & E_{\mathbf{k}} & 0 & G_{\mathbf{k}}^* \\ H_{\mathbf{k}} & F_{\mathbf{k}} & C & I_{\mathbf{k}} & G_{\mathbf{k}} & 0 \\ 0 & E_{\mathbf{k}}^* & I_{\mathbf{k}}^* & A & D_{\mathbf{k}}^* & H_{\mathbf{k}}^* \\ E_{\mathbf{k}} & 0 & G_{\mathbf{k}}^* & D_{\mathbf{k}} & B & F_{\mathbf{k}}^* \\ I_{\mathbf{k}} & G_{\mathbf{k}} & 0 & H_{\mathbf{k}} & F_{\mathbf{k}} & C \end{pmatrix} \quad (16)$$

with

$$\begin{aligned} A &= [-S(J + 2J')(\cos \alpha_{1,2} + \cos \alpha_{1,3}) + H \cos \alpha_1], \\ B &= [-S(J + 2J')(\cos \alpha_{1,2} + \cos \alpha_{2,3}) + H \cos \alpha_2], \\ C &= [-S(J + 2J')(\cos \alpha_{2,3} + \cos \alpha_{1,3}) + H \cos \alpha_3], \\ D_{\mathbf{k}} &= S(\cos \alpha_{1,2} + 1)\gamma_{\mathbf{k}}^{(1)}/2, \quad E_{\mathbf{k}} = S(\cos \alpha_{1,2} - 1)\gamma_{\mathbf{k}}^{(1)}/2, \\ F_{\mathbf{k}} &= S(\cos \alpha_{2,3} + 1)\gamma_{\mathbf{k}}^{(1)}/2, \quad G_{\mathbf{k}} = S(\cos \alpha_{2,3} - 1)\gamma_{\mathbf{k}}^{(1)}/2, \\ H_{\mathbf{k}} &= S(\cos \alpha_{1,3} + 1)\gamma_{\mathbf{k}}^{(2)}/2, \quad I_{\mathbf{k}} = S(\cos \alpha_{1,3} - 1)\gamma_{\mathbf{k}}^{(2)}/2. \end{aligned} \quad (17)$$

where  $\gamma_{\mathbf{k}}^{(1)}$  and  $\gamma_{\mathbf{k}}^{(2)}$  are given by

$$\begin{aligned} \gamma_{\mathbf{k}}^{(1)} &= J e^{i\mathbf{k}(\mathbf{a}+\mathbf{b})} + J' (1 + e^{i\mathbf{k}(-\mathbf{a}+2\mathbf{b})}), \\ \gamma_{\mathbf{k}}^{(2)} &= J e^{i\mathbf{k}(-\mathbf{a}+2\mathbf{b})} + J' e^{i\mathbf{k}(\mathbf{a}+\mathbf{b})} (1 + e^{i\mathbf{k}(-\mathbf{a}+2\mathbf{b})}). \end{aligned} \quad (18)$$

The additional term  $\Delta_{\mathbf{k}}$  in Eq. (4) of the main text is given by  $\Delta_{\mathbf{k}} = A + B + C$ .

*uud state* — The *uud* state also belongs to the family of coplanar states. Hence the expressions for the classical energy and for the coefficients of the fluctuation Hamiltonian (Eqs. (13), (16) and (17)) obtained previously can be applied to the *uud* state if one replaces  $\alpha_1 = \pi$  and  $\alpha_2 = \alpha_3 = 0$ .